LONGITUDINAL AND LATERAL STRUCTURE OF ELECTROMAGNETIC CASCADES SIMULATED BY FULL MONTE-CARLO METHOD

By E. Kryś

Institute of Physics, University of Łódź*

(Received June 8, 1984; final version received September 14, 1984)

Results of Monte-Carlo simulation of electromagnetic cascade development in the atmosphere are analysed. It is demonstrated that, whereas the longitudinal development is well described by commonly used analytical formulae, the simulated lateral distributions are clearly narrower than those obtained from the so-called Nishimura-Kamata-Greisen formulae. The deviations from those formulae are in fact more complicated. The lateral distributions of electrons in showers of a fixed age depend both on the level of shower starting point and on primary energy.

PACS numbers: 94.40.Pa, 13.85.Tp

1. Introduction

The present work concerns the investigation of the electromagnetic cascades in air. The investigations were performed by the analysis of cascades simulated using the Monte-Carlo method. The simulations were based on the detailed modelling of a three-dimensional propagation of particles allowing for all processes in which particles may participate.

The interest in electromagnetic cascades results mainly from the fact that their properties determine the picture of extensive air showers (EAS). Though the lateral distributions of electrons in EAS are not identical with those in cascades they are closely determined by the latter and the knowledge of them is indispensable for the proper estimation of main EAS parameters such as a number of particles or an age parameter.

The other very important problem in which the knowledge of electron lateral distributions is necessary is that of multicore air showers. The additional cores in showers are most probably results of the so-called jets, produced in quark-quark or possibly quark-gluon scattering. The knowledge of electron lateral distributions is necessary to estimate jet energy because it is made on the basis of only small fraction of all electrons originated

* Address: Instytut Fizyki, Universytet Łódzki, Nowotki 149/153, 90-236 Łódź, Poland.

in the jet. Because of the fundamentality of this problem, the investigation of the structure of central part of EAS is of special importance.

The widely applied to electron lateral distributions NKG-formulae were obtained on the basis of so-called diffusion equations satisfied by functions describing the changes of electrons and photons energy spectra in an absorber. The existing solutions of diffusion equations were obtained by use of a simplified model of the electromagnetic cascade development. In this model many physical processes, except the electron positron pair creation, bremstrahlung, ionisation losses and Coulomb scattering of charged particles were not taken into account and for the regarded ones the asymptotic formulae for cross sections were used.

The investigations of electromagnetic cascade by use of Monte-Carlo method bagan in 1975 after the first signals indicating that the generally used NKG curves are probably inaccurate. The sugestion presented by Allan [1] that lateral distributions are significantly narrower caused a special interest because it was stated independently in mountain experiments (Mt. Chacaltaya and Tien-Shan) that so-called age parameter of EAS obtained on the basis of the used lateral distribution function was surprisingly small: smaller than unit, although the considered showers were well below maximum in their development. These facts caused that in a number of centres the detailed investigations of the electromagnetic cascade development were undertaken.

2. Outline of the results obtained from the solutions of diffusion equations

The existing solutions of diffusion equations are obtained under simplifying assumptions concerning the electromagnetic cascade development. In a case of the one-dimensional cascades two approximations (A and B) were used. In the approximation A only the electron-positron pair creation and bremstrahlung processes are allowed for, and in the approximation B the ionisation losses of electron are additionally included. Under such assumptions the electromagnetic cascade development does not depend on the absorber.

The longitudinal development of cascades is described by the cascade curves, that is to say by the total number of particles (electrons or photons) with energy above some threshold at different depths in an absorber. The cascade curves in these approximations were obtained analytically and are of the form:

$$\text{in the approximation } A\text{: } N(>E, E_0, t) = f\left(\frac{E_0}{E}, s\right),$$

$$\text{in the approximation } B\text{: } N(>E, E_0, t) = f\left(\frac{E_0}{\mathscr{E}_k}, \frac{E}{\mathscr{E}_k}, s\right)$$

(see Bielenki [2]). The allowance for other processes makes the diffusion equations so complicated that their analytical solutions become impossible.

The spatial development of particles in a cascade was obtained from diffusion equations in the approximation B modified by adding to one-dimensional equations a new part describing the lateral development of particles due to the Coulomb scattering of charged

particles. In many theoretical calculations based on the analysis of diffusion equations only the moments of distributions were obtained and in the process lateral structure function of particles was fitted to these moments. The most popular fit to the moments was found by Nishimura and Kamata and the Greisen curves (NKG formulae). These curves describing the lateral development of particles in a cascade at a some depth in an absorber are only dependent on the age parameter of cascade which shows at what stage of development the cascade is observed:

$$f\left(\frac{r}{r_1}\right) = C(s)\left(\frac{r}{r_1}\right)^s\left(1+\frac{r}{r_1}\right)^{s-4.5}, \tag{1}$$

where s is defined by equation: $s = \dfrac{3t}{(t+2\beta)}$, t being here the depth in radiation lengths and $\beta = \ln\dfrac{E}{\varepsilon_k}$ and $\varepsilon_k = 76$ MeV; r_1 is the Molier unit; $C(s) = \dfrac{\Gamma(4.5-s)}{2\pi\Gamma(s)\Gamma(4.5-2s)}$.

The first Monte-Carlo simulations of electromagnetic cascades by Allan [1] and Hillas [3] showed that the lateral distributions of particles are significantly narrower than those expected from NKG formulae. For a few years the detailed simulations of electromagnetic cascades in air were performed in Łódz and the summary is presented in this paper

3. Assumptions in the model of electromagnetic cascades in air used in these calculations

The main factors having directly an effect on the electromagnetic cascade development are cross sections for all physical processes in which particles are involved and also the model of the atmosphere. These quantities determine the electromagnetic cascade development in air.

3.1. The model of the atmosphere and the radiation unit

The atmosphere is the medium in which the density changes with height (essentially pressure and temperature). In simulation of electromagnetic cascades in air a variation of the density with altitude was taken according to the formulae:

$$h = 44308\left(1-\frac{p}{p_0}\right)^{0.1903} \quad \text{for} \quad h \leqslant 11\text{ km},$$

$$h = 11000+6340\ln\left(\frac{p_{11}}{p}\right) \quad \text{for} \quad 11\text{ km} < h < 30\text{ km}, \tag{2}$$

where p_0 and p_{11} are the pressures on the height of 0 and 11 km above sea level respectively. For the greater heights the satellite measurements were taken.

The mass composition was used as:

	%	A
N_2	78.09	28.00
O_2	20.95	32.00
Ar	0.93	39.94
CO_2	0.03	44.01

The characteristic unit used to express the thickness of air in a case of electromagnetic processes is the radiation unit t_0. In air it can be obtained from:

$$\frac{1}{t_0} = \tfrac{4}{137} r_0^2 Z(Z+\xi) \frac{N_0}{A} [\ln (183\, Z^{-1/3}) - f(Z)], \tag{3}$$

where $f(Z) = 0.00347$, $\xi(Z) = 1.3075$, $Z = 7.37$ (average atomic number), $A = 14.74$ (average mass number), N_0 = Avogadro number, r_0 = classical electron radius. This equation gives $t_0 = 36.4$ g/cm^2.

3.2. Radiation and pair creation

The cross section for bremstrahlung and pair creation were taken in the form:

bremstrahlung:

$$d\phi = 4\alpha r_0^2 Z(Z+\xi) \frac{d\varepsilon}{\varepsilon} \{[1+(1-\varepsilon)^2] [\tfrac{1}{4} f_1(\delta) - \tfrac{1}{3} \ln Z - f(Z)]$$

$$- \tfrac{2}{3} (1-\varepsilon) [\tfrac{1}{4} f_2(\delta) - \tfrac{1}{3} \ln Z - f(Z)]\}, \tag{4}$$

pair production:

$$d\phi = 4\alpha r_0^2 Z(Z+\xi) d\{[(\varepsilon^2+(1-\varepsilon)^2] [\tfrac{1}{4} f_1(\delta) - \tfrac{1}{3} \ln Z - f(Z)]$$

$$+ \tfrac{2}{3} \varepsilon(1-\varepsilon) [\tfrac{1}{4} f_2(\delta) - \tfrac{1}{3} \ln Z - f(Z)]\}. \tag{5}$$

The screening functions $f_1(\delta)$ and $f_2(\delta)$ are expressed in terms of the parameter delta:

bremstrahlung:

$$\delta = \frac{136}{Z^{1/3}} \frac{\varepsilon}{E_0(1-\varepsilon)}, \quad \varepsilon = \frac{k}{E_0}, \tag{6}$$

pair production:

$$\delta = \frac{136}{Z^{1/3}} \frac{1}{k_0(1-\varepsilon)\varepsilon}, \quad \varepsilon = \frac{E}{k_0}, \tag{7}$$

where E_0, k_0 — the primary energy of particle. The functions $f_1(\delta)$ and $f_2(\delta)$ have the form:

$$\begin{aligned} f_1(\delta) &= 20.867 - 3.24\delta - 0.625\delta^2, \\ f_2(\delta) &= 20.209 - 1.93\delta - 0.086\delta^2, \end{aligned} \quad \text{for} \quad \delta \leqslant 1,$$

$$f_1(\delta) = f_2(\delta) = 21.12 - 4.184 \ln (\delta + 0.952) \quad \text{for} \quad \delta > 1. \tag{8}$$

In the asymptotic case of the complete screening of the nucleus Coulomb field by the atomic electrons ($\delta \to 0$) as used in the diffusion equations this functions are:

$$f_1(0) = 4 \ln 183, \quad f_2(0) = 4 \ln 183 - \tfrac{2}{3}. \tag{9}$$

The angle of emission between the photon and secondary electrons is given by Stearns [4] in a form:

$$\sqrt{\langle\theta^2\rangle} = f(\varepsilon, Z)\frac{\ln E_0}{E}. \tag{10}$$

The angle of emission between either of the secondary particles and the primary track in pair production is given as:

$$\sqrt{\langle\theta^2\rangle} = g(\varepsilon, Z)\frac{\ln E}{E}. \tag{11}$$

3.3. Inelastic scattering of electrons and positrons with production of delta electrons

Electron or positron while passing through a medium can collide with atomic electrons. There is difference between the cross-section for primary electrons and positrons because of the indistinguishability of the primary and secondary electrons in the first case. The cross-sections for the inelastic scattering of electron called Molier scattering is given by formula:

$$d\Phi = \frac{2\pi r_0^2}{\beta_0^2}\frac{d\varepsilon}{\varepsilon}\left[\frac{1}{\varepsilon^2} + \frac{1}{(1-\varepsilon)^2} + \frac{T_0^2}{E_0^2} - \frac{2T_0+1}{E_0^2}\cdot\frac{1}{\varepsilon(1-\varepsilon)}\right], \tag{12}$$

where T_0, T — electron kinetic energy, $\varepsilon = T/T_0$.

The cross-section for inelastic positron scattering (Bhabha scattering) is given by the formula:

$$d\Phi = \frac{2\pi r_0^2}{\beta_0^2}\frac{d\varepsilon}{T_0}\left\{\frac{1}{\varepsilon^2} - \beta^2\left[(2-y^2)\frac{1}{\varepsilon} - (3-6y-y^2-2y^3)\right.\right.$$

$$\left.\left. + (2-10y+16y^2-8y^3)\varepsilon - (1-6y+12y^2-8y^3)\varepsilon^2\right]\right\},$$

where

$$y = \frac{1}{T_0+2} \quad \text{and} \quad \beta_0^2 = 1-\frac{1}{E_0^2}. \tag{13}$$

The total cross-section for the electron scattering is larger than for positron scattering at energies lower than a few MeV, and for the higher energies they are the same. The angles between the direction of the primary and direction of the secondary electrons of energy T are:

$$\cos\theta = \sqrt{\frac{(T_0+2)T}{T_0(T+2)}}. \tag{14}$$

3.4. Ionisation losses

In the present work the rate of energy loss per track length was expressed as:

$$\frac{dE}{dt} = a - b_i E^{-\gamma_i}, \quad i = \text{e, p (electron, positron)},$$

where the constants a, b and γ depend only on the atomic number of medium. The constans a, b and γ for air have values:

$$a = 147.550, \quad b_e = 72.13, \quad b_p = 67.24,$$

$$\gamma_e = 0.384, \quad \gamma_p = 0.324,$$

(if E is expressed in units of electron rest energy).

3.5. The Coulomb scattering

The used form of the cross-sections of any electron deflected at an angle θ and $\theta + d\theta$ after traversing a layer of matter is based on Molier's scattering theory with the second term of his equation as given by Molier [5] in the form:

$$f(\theta)d\theta = \left(\frac{\sin\theta}{\theta}\right)^{1/2} [f^{(0)}(\Phi) + B^{-1} f^{(1)}(\Phi)] \Phi d\Phi, \tag{15}$$

where Φ is the reduced angle of θ defined as:

$$\Phi = \frac{\theta}{\chi_c \sqrt{B}}, \quad \chi_c^2 = 4\pi r_0^2 t_0 \frac{\varrho Z^2 N_0}{A} \int_0^t \frac{dt}{\beta^2 E^2}.$$

The parameter B is defined by the transcendental equation:

$$B - \ln B = B', \quad B' = \ln \frac{\chi_c^2}{1.167\,\chi_a^2},$$

$$\chi_a^2 = 6.8 \cdot 10^{-5} Z^{2/3} [1.13 + 3.76(\tfrac{1}{137} Z)^2] \frac{1}{\beta^2 E^2},$$

$$\beta^2 = 1 - \frac{1}{E^2}.$$

The first term represents the effect of multiple scattering, the second one the effect of single scattering. The functions $f^{(0)}(\Phi)$ and $f^{(1)}(\Phi)$, were also taken after Molier [5].

3.6. The Compton effect

The cross-section is given by the Klein-Nishina formula:

$$d\Phi = \pi r_0^2 \frac{d\varepsilon}{k_0 \varepsilon} \left\{ 1 + \varepsilon^2 - \frac{2}{k_0^2}(1 + k_0) + \frac{\varepsilon}{k_0^2}(1 + 2k_0) + \frac{1}{k_0^2 \varepsilon} \right\}, \tag{16}$$

where $\varepsilon = k/k_0$.

For each secondary particle the energy and momentum conservation laws give limits for the angles of emission:

$$\cos\theta_1 = 1 - \frac{1}{k} + \frac{1}{k_0}, \tag{17}$$

$$\sin\theta_2 = \frac{k\sqrt{1-\cos^2\theta_1}}{\sqrt{(k_0-k)(k_0-k+2)}}, \tag{18}$$

where θ_1 is the angle between direction of primary and secondary photon, θ_2 is the angle between the primary photon and electrons and k_0, k are expressed in units of electron rest energy.

3.7. The photo-electric effect

The following approximation of the total cross-section obtained on the basis of Pratt theory [6] was used in these calculations:

$$\Phi = \Phi_0(b_0 + b_1 k^{-1} + b_2 k^{-2}) f(a), \tag{19}$$

where $\Phi_0 = 4\pi r_0^2 a^4 \frac{Z}{k}\frac{\varrho N}{A}$ and b_0, b_1, b_2, $f(a)$ depends on $a = \alpha Z$.

4. Results

The simulation of the electromagnetic cascades was made for:
— two depths from the starting point of cascades in the atmosphere,
— different primary energies.

4.1. Longitudinal development of the electromagnetic cascades

The results are presented in Fig. 1 where cascade curves are plotted. Cascade curve represents the number of particles above fixed energy threshold as a function of depth in absorber. The results of simulation are compared with curves obtained by the solution of the diffusion equations in the approximation B. The cascade curves in these figures for the secondary electrons (solid line) and for the secondary photons (dashed line) are taken according to the analytical solutions by Bielenki [2]. They are shown separately for the cascades passing throught all the atmosphere and for the cascades initiated on the depth of 712 g/cm^2 (for this case the change of atmosphere density is rather small).

It can be seen that there is good agreement between the numbers of electrons and photons obtained from our simulation and the numbers of particles calculated on the basis of the analytical solutions of the diffusion equation in the approximation B. Additionally, the comparison of these curves with the points shows that there is no significant difference in a shape of the cascade curves for both levels of the initiating points.

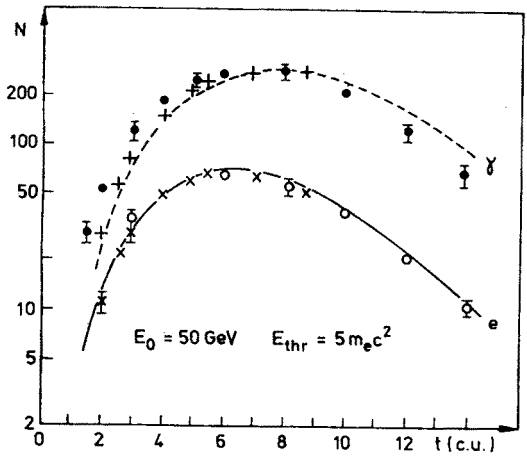

Fig. 1. The longitudinal development of electromagnetic cascades. The points are the values from simulation for the two starting points of the cascades: circles refer to the top of the atmosphere, crosses — to the depth of 712 g/cm^2. The curves are obtained analytically under approximation B (solid line corresponds to electrons, dashed — to photons)

Recapitulating this section we can say, that longitudinal development of the electromagnetic cascades in air is well described by the analytical solution of diffusion equation in approximation B.

4.2. Lateral development of the electromagnetic cascades

4.2.1. Dependence of the lateral distribution of secondary electrons on the depth of initiation point in air

Up to now, it was always assumed that the lateral distribution of particles expressed in Molier units depends only on one parameter which describes longitudinal development of cascades, i.e. the age parameter. It means, that for the same stage of development of cascades the distributions of particles at different depths in the atmosphere should be identical. In Fig 2 one can see the calculated values of the mean distances of secondary particles from the cascade axis versus depth of development of cascades. This dependence is shown for both above mentioned cases, namely for the cascades initiated at the depth of 712 g/cm^2 and at the top of atmosphere for primary energies of 10 GeV. As one can see the mean distance of particles from the cascade axis (width of the lateral distributions) depends on the starting point of cascade in the atmosphere for the same stage of the development of the cascade.

From these facts one can conclude that the change of density of air has an effect on the width of the lateral distribution (we call it the density effect). The width of lateral distribution becomes larger with the larger density gradient in the atmosphere. It means that the larger height of production of particles (for cascades initiated higher in the atmosphere) relates to the wider lateral distribution. It is clearly seen in Fig. 3 where the lateral distributions of electrons in cascades initiated at different depths in the atmosphere are presented. These discrepancies may result from the fact that the Molier unit characteristic of the observation level was used, while actually the cascade developes in the same layer

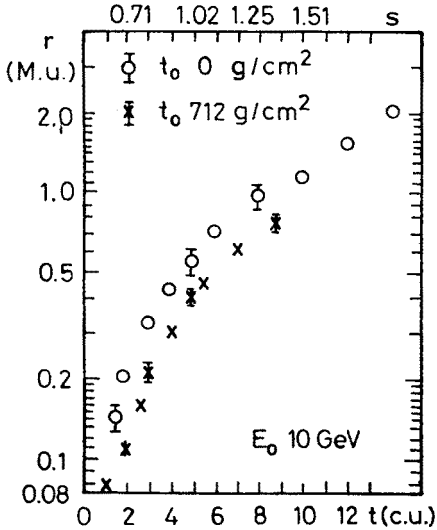

Fig. 2. Mean radii of the electromagnetic cascades as a function of depth for two different levels of cascade origin

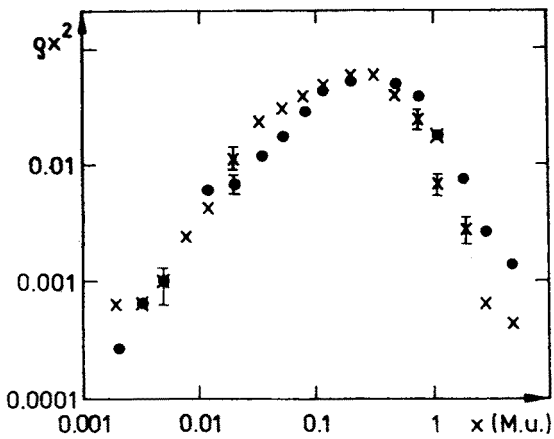

Fig. 3. Lateral distributions of all secondary electrons (above 1 MeV) in the cascades initiated by primary photon of energy 50 GeV at the depth of 5 c.u. beyond the starting point. The two starting points of cascades are shown: crosses — the depth of 712 g/cm^2, circles — the top of the atmosphere. ϱ is the density of electrons (including positrons). $X = \frac{r}{r_1} \cdot \varrho x^2$ is normalized to one particle in the cascade on this level

of air above this level, where the density of air is smaller and changing continuously. The analysis of the simulation data has shown that in a case of air absorber the differences in lateral distributions of electrons can be eliminated by recalculating these distributions for the uniform height above the observation level called in the process "the effective height". This height was found by us to be equal to approximately two cascade units. The

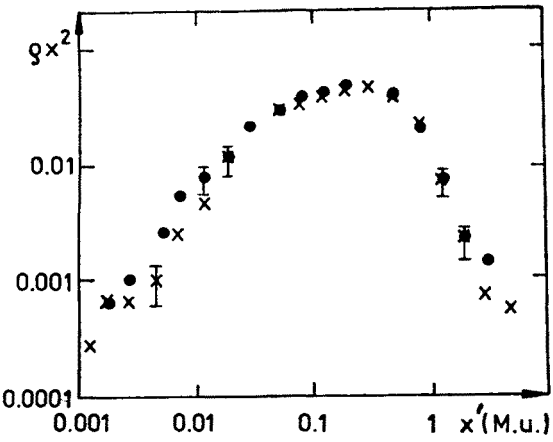

Fig. 4. Lateral distributions of all secondary electrons (see Fig. 3) for the observation level of 5 c.u. below the initiating point, transformed to the effective height

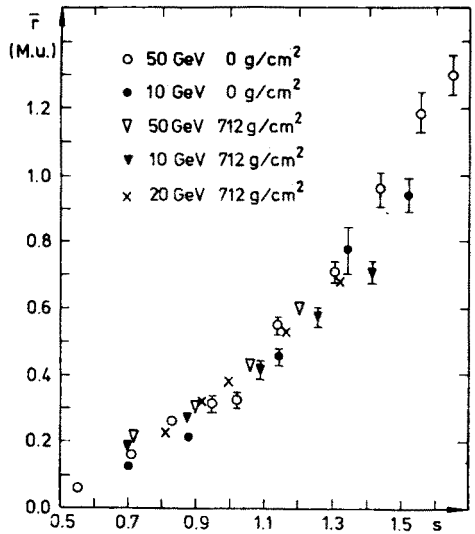

Fig. 5. The mean radii recalculated for effective height as a function of the age parameter for three primary energies 10 GeV, 20 GeV, 50 GeV and the two starting points of the cascades at the top of atmosphere and at the depth of the 712 g/cm²

new Molier unit $\left(x' = x \cdot \frac{\eta(t-2)}{\eta(t)}\right)$ is greater than the one corresponding to the observation level by a factor equal to the quotient of the densities of air at these two levels. This is visible in Fig. 4 where there are shown the distributions of electrons for the primary photon of energy of 50 GeV and for the observation level of 5 c.u. below the initiating point, transformed to the effective height. The agreement is also visible in Fig. 5 where the mean distances of secondary particles recalculated for certain effective height of 2 c.u. for three primary energies and several observation levels (below 3 c.u.) are shown.

The presented results show that the satisfactory agreement between the lateral distributions of particles in cascades initiated at different depths in the atmosphere can be achieved by transforming them to the effective height of two cascade units above the observation level.

4.2.2. Lateral distributions of electrons and the primary particle energy

The analysis of the simulation data has shown that the lateral distributions of electrons in cascades at the same stage of development depend on the primary particle energy. Because of the density effects in the air this dependence is rather complicated. However, when recalculated for the "effective height" the distributions show clear tendency to become wider with increasing energy. It is seen in Fig. 5 where the recalculated mean radii are plotted versus age parameters for three primary energies 10 GeV, 20 GeV, 50 GeV and the two starting points of the cascades: at the top of atmosphere and at the depth of 712 g/cm^2. It is seen, that the widths of distributions are increasing with energy of the primary particles. It is estimated that the mean radius increases of about 10% if the energy of primary particle changes from 10 GeV to 50 GeV.

From these facts one can conclude that the primary particle energy has an effect on the estimation of the age parameter from the lateral structure function.

4.2.3. The comparison of simulation of the electromagnetic cascades with the other results

It has been pointed out by several authors that the electron lateral distributions in electromagnetic cascades cannot be well described by the NKG formula.

The Hillas approximation [3] of the lateral distributions of electrons obtained on the basis of simulation of the electromagnetic cascades in air and the theoretical approximation of Uchaikin [7] based on the numerical solution of the diffusion equation show that the lateral distributions are narrower than those predicted by the Greisen formula.

Comparison of our results obtained for two different cascade starting points in atmosphere with the Hillas and the NKG curves is shown in Fig. 6. As it is visible in Fig. 6 our lateral distributions are narrower when compared with the Greisen formulae with the age parameter taken from the longitudinal development, and especially for the cascades initiated deep in the atmosphere. The present situation as illustrated in Fig. 6 is such that at small distances from the cascade axis evident differences between the curves exist. The Hillas results and our simulation indicate that at small distances from the core the lateral distributions of particles are flatter than it was thought up to now and they are steeper at large distances. The Uchaikin formula was obtained for particles at distances greater than 2 m and cannot be used for the nearer ones. At large distances they agree with the Hillas curves. It means that the number of particles near the axis as calculated from the NKG formula was overestimated.

These deviations have significant consequences for the experimental investigations of high energy cosmic rays. For instance the flat distributions of electrons at small distances from the axis would lead to underestimation of the energy in subcores in EAS.

It seams useful to check whether the lateral distributions at distances greater than 0.1 M.u. can be described by the NKG formula with the parameter different from the age

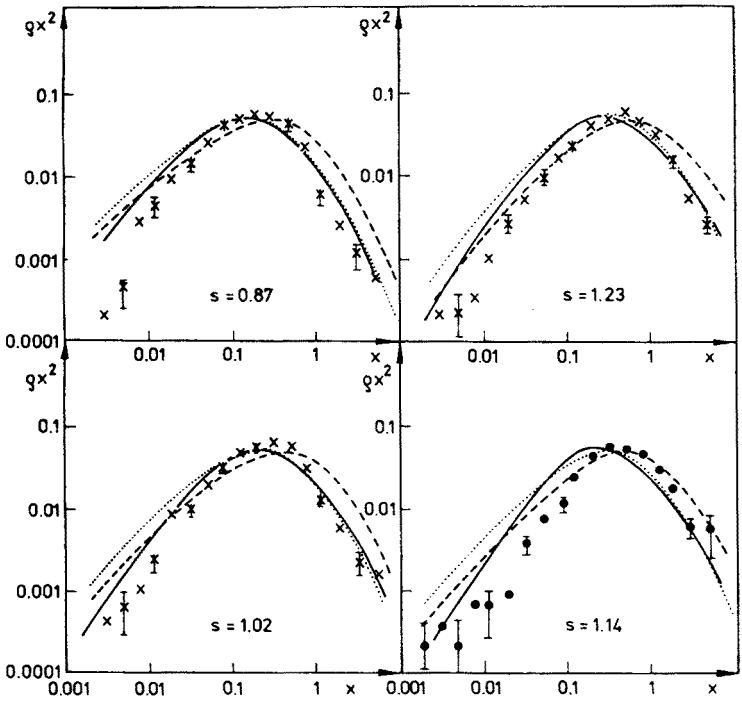

Fig. 6. Lateral distributions of electrons. The points are simulation, the curves are: ——— NKG functions, ——— Hillas formulae and ····· Uchaikin formulae. The two starting points of the cascades: crosses — the depth 712 g/cm², circles — the top of atmosphere

parameter describing the longitudinal development. Let us analyse the so-called local age parameter of a cascade defined as the age parameter obtained from the NKG formulae on the basis of the particle density in two distances from axis.

The value of the local age parameter determined from our data (Fig. 7) changes from a value clearly greater than the age parameter at small distances to the value significantly lower than the age parameter at distances greater than 0.1 Molier unit. It means that the lateral distributions of particles obtained on the basis of simulation of the electromagnetic cascade cannot be described by the Greisen formula — even with the parameter different from the age parameter. In the other words the lateral distributions have the shape different from those given by the Greisen formula.

Let us examine the influence of width and shape of the lateral distributions of the electromagnetic cascade on the EAS data interpretation. In the EAS research widely applied is the method estimation of fundamental parameters (i.e. age parameter and a number of particles) based on the assumption that lateral distributions of particles in air showers are of the same type as in the electromagnetic cascades. In EAS experiment we cannot measure directly the lateral distribution of particles. The lateral distributions are always reconstructed by fitting the NKG function to the experimentally measured density of particles at several distances from the shower axis.

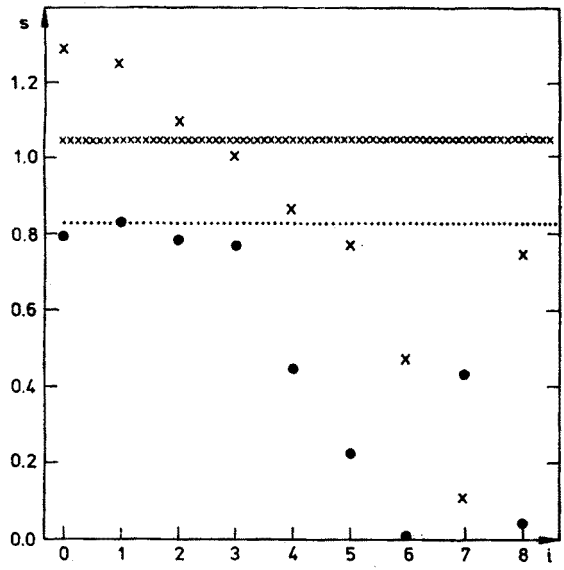

Fig. 7. The value of the local age parameter as a function of distance R_i from the cascade axis. R_i is defined as $R_i = r_1 \cdot 10^{(-1.1+0.2i)}$, where r_1 is Molier unit. The local age parameter at the distance of R_i is obtained from the NKG formulae on the basis of ratio of electron densities in two distances from axis R_{i-1} and R_i

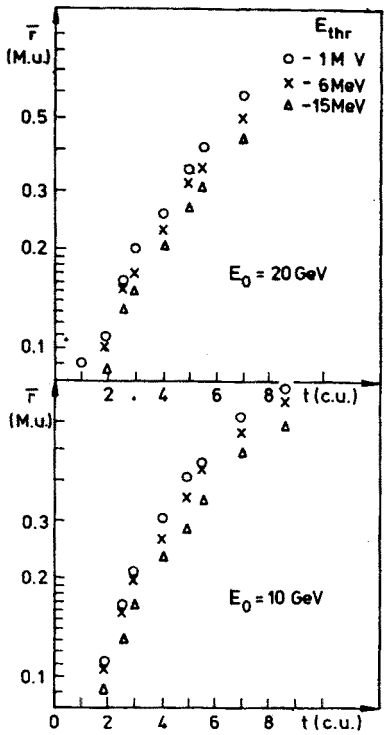

Fig. 8. The values of mean radii of electrons with threshold of 1 MeV, 6 MeV and 15 MeV

As it was pointed out in this paper the NKG function does not describe well the lateral distributions of particles in the individual cascades. It is probable that the signalized incoherences in EAS research (i.e. change of the age parameter with distance) can be explained as a result of employing the incorrect formula (i.e. the NKG one) for lateral distributions in showers.

4.2.4. Lateral distributions of electrons with various energetical threshold

In simulation of electromagnetic cascades the lateral distributions were calculated for various energetical thresholds. The mean distances form the axis of secondary electrons with the energy threshold of 1 MeV, 6 MeV, 15 MeV versus age parameter are shown in Fig. 8. One can see that the values of mean radii of electrons with thresholds of 6 MeV and 15 MeV are smaller by 10% and 25%, respectively, than the radii for the electrons with 1 MeV threshold. However, it is naturally expected that the lateral distributions of electrons with higher threshold are narrower.

In most experiments the shower particles are detected only if their energy exceeds some threshold. This effect leads to further reduction of the experimentally determined age parameter (for instance in a case of the threshold of 15 MeV the underestimation of the age parameter amounts to $\Delta s = 0.1$).

5. Conclusions

On the basis of our simulation results we conclude that:

1. The longitudinal development of cascades agrees well with the analytical solutions in the approximation B and does not depend on the starting point of development of the cascade.
2. The lateral distributions of particles are clearly narrower than the NKG distributions with the age parameter describing longitudinal development of the cascades.
3. It is not possible to describe the lateral distribution of all particles with NKG formula and the "age parameter" independent of the distance from the axis. At small distances from the cascade axis the lecal age parameter is greater than that obtained from the lengitudinal development (Fig. 7). At larger distances it is lower. The method of describing lateral distributions of electrons by the NKG function with one local parameter as used in EAS experiments can lead to different results depending on distances at which this parameter is estimated.
4. It is an interesting result of the present simulation that the lateral distributions of particles at small distances from the cascade axis are flatter than the NKG ones. It means that the number of particles obtained from the NKG formula is overestimated.
5. In the present work lateral distributions of particles for different energy thresholds were analysed. As could be expected the distributions appeared narrower for secondary particles with higher energy threshold.
6. It was stated that initiating point of the cascade development in air has an effect on the width of electron lateral distribution. It appeared, however, that the width of distribution

is determined by the density of atmosphere at so-called effective height above the considered level and this gives the possibility to remove the differences in shape of the distributions. On the basis of the simulation results the effective height was estimated as being equal to two cascade units.

7. The investigation of the effect of primary particle energy on the width of electron lateral distribution shows that the mean distance of particles from the cascade axis corrected to the density effect increases with the primary particle energy.

The author would like to express the sincere thanks to Prof. J. Wdowczyk from the Institute of Nuclear Studies for helpful discussions and continuous support of this work. She is also greatly indebted to her colleague from the Institute of Nuclear Studies Mr. A. Wasilewski for fruitful cooperation in programming and analysing the results.

REFERENCES

[1] H. Allan et al., XIV ICRC, Munich **6**, 3071 (1975).
[2] S. Z. Bielenki, I. P. Ivanienko, *Usp. Fiz. Nauk* **69**, 591 (1958).
[3] A. M. Hillas, J. Lapikens, XV ICRC, Plovdiv **8**, 460 (1977).
[4] M. Stearns, *Phys. Rev.* **76**, 826 (1949).
[5] G. Molier et al., Kos. Strahlung, Berlin 1953.
[6] R. M. Pratt, *Phys. Rev.* **117**, 1017 (1979).
[7] V. V. Uchaikin et al., XVI ICRC, Kyoto **7**, (1979).